Convexity of the effective potential

M Hindmarsh and D Johnston

The Blackett Laboratory, Imperial College, London SW7 2BZ, UK

Abstract. We show that an interpolated loop expansion produces a convex effective potential for Higgs fields in the vector representations of $SU(N)$ and $SO(N)$ and the adjoint representation of any simple Lie group, provided one considers the Higgs fields as a sector of a gauge theory and uses the gauge fixing freedom to choose a 't Hooft-type gauge fixing term. We consider the adjoint case in some detail, exploiting the correspondence between the Dynkin diagrams used to classify the symmetry breaking and the Coexeter graphs that describe the symmetries of regular polytopes to determine the shape of the linearly interpolated regions that appear in the true, convex effective potential.

1. Introduction

The effective potential V, as was pointed out by Iliopoulous *et al* (1975), is a convex function, i.e.

$$V(\bar{\Phi} + (1-\lambda)\bar{\Psi}) \leq V(\bar{\Phi}) + (1-\lambda)V(\bar{\Psi})$$

$$0 \leq \lambda \leq 1 \qquad \forall \bar{\Phi}, \bar{\Psi} \text{ (classical fields)}. \tag{1.1}$$

Explicit perturbation theory calculations, as pioneered by Jackiw (1974), use the loop expansion and vacuum graph formula

$$\Gamma(\bar{\Phi}) = U(\bar{\Phi}) + \Sigma \tag{1.2}$$

where Γ is the effective potential, U the classical potential, and Σ is the sum of vacuum graphs in the theory with the Lagrangian shifted by $\bar{\Phi}$. However, this approach produces a non-convex effective potential, which we will call 'V' to indicate its dubiety, in theories with a non-convex U. The 'V' also suffers from the disease of becoming complex inside the points of inflection of U.

The reason for the apparent disagreement between the formal convexity property and the result of the loop calculations is that the loop expansion, and consequently the vacuum graph formula, break down for certain ranges of $\bar{\Phi}$ when one has a non-convex V. The regions where 'V' becomes complex are contained within these. Fujimoto *et al* (1983) proposed a solution to these problems by taking into account the effect of competing saddle points from all the classical minima in the case of a theory with non-convex U. The net result is that the correct V is produced by linear interpolations across the non-convex regions of 'V'. This is in agreement with the arguments of Haymaker and Perez-Mercader (1984) which were based on analogy with statistical mechanics. They deduced that the non-convex regions of 'V' corresponded to higher energy branches of the ground-state energy of the combined system and
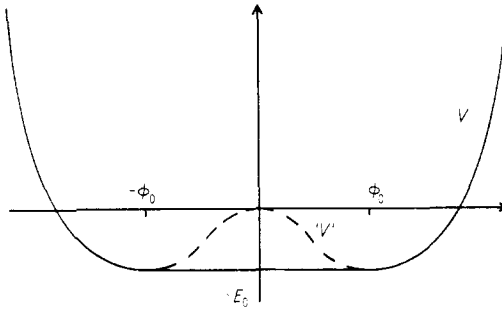
Figure 1. The effective potential for a ϕ^4 theory. 'V' is the potential calculated in a loop expansion, and V is the convexified version. The region between $-\phi_0$ and ϕ_0 corresponds to a superposition of the two ground states with energy E_0 based at $\pm\phi_0$.

source. V is produced by taking the locus of the tangent (hyper) planes to 'V'. Lattice calculations (Callaway and Maloof 1983, Do Amaral *et al* 1984) support the interpolated form of V, as does the application of Wilson recursion relation (Fukuda 1976) (see figure 1). It would, of course, be more satisfactory to derive V initially instead of patching up 'V'. In this paper we follow the philosophy of Fujimoto *et al*, who considered $\lambda\Phi^4$, by taking account of the various classical minima and obtaining V directly. We consider Higgs fields in the adjoint representation of any simple Lie group and the vector representation of SO(N) and SU(N).

The paper is divided up as follows. In § 2, as a preliminary to demonstrating convexity we discuss the linearly interpolated, or convexified, regions of V and how they are produced. In § 3 we consider the behaviour of $\bar{\Phi}$, the classical field, as a function of the external source J and we show how, provided we have separated classical minima, the non-convex portions of 'V' are excised. In § 4 we show that this separation may be achieved by assuming that we are working with the Higgs sector of a gauge theory and using a 't Hooft-style gauge fixing

$$-(1/2\alpha)(\partial_\mu A^\alpha_\mu - iT^\alpha_{ij} w_i \Phi_j)^2 \tag{1.3}$$

where T^α_{ij} is a generator of the gauge group and w_j is an arbitrary vector in the Higgs representation space. This reduces the manifold of minima G/H to a discrete set of points, which allows us to apply the arguments of § 3. We also show that the convexified region in the vector case is analogous to $\lambda\Phi^4$, as the gauge condition corresponds to taking a one-dimensional slice through the manifold of minima, which is a hypersphere. The adjoint case, however, is more subtle and we consider it in some detail in § 5, where we show that the convexified region is a polytope whose dimension depends on the direction of the external source J and whose size depends on its magnitude J. This is the result of the correspondence between the Dynkin diagrams that are used to classify symmetry breaking in the adjoint representation and Coxeter graphs which classify the symmetries of polytopes (Coxeter 1948)[†]. We summarise the relevant mathematics in the appendix. In § 6 we present our conclusions.

2. Linear interpolation

In this section we will demonstrate, following Evans and McCarthy (1984), that we can construct the linearly interpolated regions of the effective potential by taking

[†] We are grateful to T W B Kibble for pointing this out to us.

quantum superpositions of the degenerate ground states, and it will emerge in § 5 that these regions in the space of the adjoint fields are just the regular polytopes as classified by Coxeter (1948).

Evans and McCarthy took a ϕ^4 theory with two degenerate vacuum states $|+\rangle$ and $|-\rangle$ at $\pm\phi_0$. For any finite volume of spacetime there will be matrix elements of observables connecting the two, as it requires a finite amount of energy to cross the hump in the potential. In the infinite volume limit, however, the matrix elements will vanish, and we may write

$$\langle\pm|H|\pm\rangle = E_0\delta_{\pm\pm} \qquad \langle\pm|\Phi|\pm\rangle = \pm\phi_0\delta_{\pm\pm} \qquad (2.1)$$

where H includes the energy of interaction with the current. Any linear combination of these states will be an equally good ground state with energy E_0, as we may see from the following:

$$|\lambda\rangle = \lambda_+|+\rangle + \lambda_-|-\rangle, \qquad \|\lambda_+\|^2 + \|\lambda_-\|^2 = 1 \qquad (2.2)$$

$$\langle\lambda|H|\lambda\rangle = (\|\lambda_+\|^2 + \|\lambda_-\|^2)E_0 = E_0 \qquad (2.3)$$

$$\langle\lambda|\Phi|\lambda\rangle = \|\lambda_+\|^2\phi_0 - \|\lambda_-\|^2\phi_0. \qquad (2.4)$$

Note that the state $|\lambda\rangle$ has a field *vev* lying between the two minima. Since the effective potential can be defined as the minimum of $\langle H \rangle$ with $\bar{\phi} = \langle\Phi\rangle$ constrained to take a spacetime constant value, we have found that its true value between $-\phi_0$ and $+\phi_0$ is E_0; i.e. a linear interpolation (figure 1). At zero temperature we may interpret a ϕ lying between the minima as a quantum superposition describing an ensemble of systems in one or other of the ground states (Glimm and Jaffe 1981)[†]. If the spacetime volume is finite, then there will be transitions between the minima and the equilibrium state must be an equal mixture of the two; this will produce a single minimum at $\bar{\phi} = 0$, a finite volume effect which shows up in path integral (Fujimoto *et al* 1983) and lattice (Callaway and Maloof 1983) calculations.

If we can take the minima to be n discrete points in $\mathbb{R}^r$, then the obvious generalisation is to consider a superposition of ground states $|a\rangle$, $a = 1, \ldots, n$, each with energy E_0, so that (2.1) become

$$\langle a|H|b\rangle = E_0\delta_{ab} \qquad \langle a|\Phi|b\rangle = \phi_0^b\delta_{ab} \text{ (no sum)} \qquad (2.5)$$

and (2.2) becomes

$$|\lambda\rangle = \sum_{a=1}^{n} \lambda_a|a\rangle, \qquad \sum_{a=1}^{n} \|\lambda_a\|^2 = 1. \qquad (2.6)$$

Again, any such state $|\lambda\rangle$ is a ground state, with energy

$$\langle\lambda|H|\lambda\rangle = E_0 \qquad (2.7)$$

and $\bar{\phi}$ given by

$$\langle\lambda|\Phi|\lambda\rangle = \sum_{a=1}^{n} \|\lambda_a\|^2\phi_0^2. \qquad (2.8)$$

This is just the convex hull of the set $\{\phi_0\}$ (see figure 2). For suitable gauge-fixed adjoint scalar theories this set will turn out to be the vertices of a regular polytope

---

[†] At finite temperature the effective potential is the Helmholtz free energy, and the minimum free energy for a particular (space averaged) $\langle\phi\rangle$ will occur for an inhomogeneous mixture as this has greater entropy than a homogeneous state.
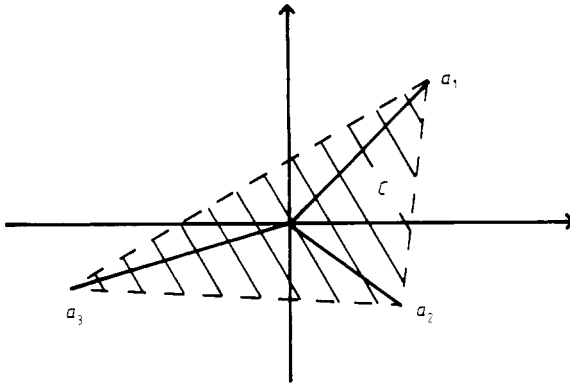
Figure 2. The convex hull C of the set of position vectors $\{a_1, a_2, a_3\}$ in $\mathbb{R}^2$, defined by $C = \{v: v = \Sigma\, t_i a_i, \Sigma\, t_i = 1\}$.

(see the appendix) and so the linearly interpolated region is just its boundary and interior.

In the next section we will find that an approximation to the functional integral shows that as J moves through a critical value (where two or more minima are degenerate in energy) $\bar{\phi}$ jumps discontinuously from one minimum to another, precisely the behaviour expected if the effective potential between them is flat rather than humped.

3. Behaviour of $\bar{\Phi}$

If we have a non-convex U the minima of $U(\Phi) - J\Phi$ are not uniquely specified for all J. For certain critical values of J, say J_c, a small variation in J will cause the absolute minimum of $U(\Phi) - J\Phi$, $^{\circ}\Phi(J)$, to jump discontinuously between the local minima Φ_0^a. For example, in the case of a symmetric double well potential in a $\lambda\Phi^4$ theory, J_c is zero and a small variation either side of this causes the absolute minimum to jump between the two local minima. To deal with this we subdivide the path integral into regions R_a, each of which contains one of the Φ_0^a (Fujimoto *et al* 1983)

$$\exp(W[J]) = \sum_a \int_{R_a} [\mathrm{D}\Phi] \exp\left[-(1/\hbar)\int (L + J\Phi)\right] = \sum_a \exp(W_a[J]) \tag{3.1}$$

where $W^a[J] = \exp[-(\Omega/\hbar)(U(\Phi_0^a) - J\Phi_0^a)] \int_{R_a} [\mathrm{D}\Phi] \exp[-(-1/\hbar)\int \Delta^a L]$

$$\Delta^a L = L(\Phi + \Phi_0^a) - L(\Phi_0^a) + J\Phi$$

$$\Omega = \int \mathrm{d}^4 x. \tag{3.2}$$

The approximation necessary to evaluate (3.1) is the extension of the regions R_a to cover the full range of Φ. We would expect the overlap error thus introduced to be exponentially small, as the $\int \Delta_a L$ are large and positive in the regions of overlap. With each R_a replaced by R (3.2) can be thought of as defining a Jackiw-style expansion for V about each $\bar{\Phi}_0^a$.

$$\exp(W[J]) = \sum_a \exp[-(\Omega/\hbar)('V'(\bar{\Phi}^a) - J\bar{\Phi}^a)]. \tag{3.3}$$

We can think of the 'V' in the exponent as being calculated to any given order in the loop expansion. Outside a critical range, $J - J_c > O(h)$ one of the terms in the summation will dominate and we recover the standard loop expansion, which is acceptable as we are outside the non-convex region. Inside the critical range we need to consider the full summation. Thus to evaluate $\bar{\Phi}$ in this interval we consider

$$\bar{\Phi} = \hbar \frac{\delta W}{\delta J} = \sum_a \bar{\Phi}^a \exp[-(\Omega/\hbar)('V'(\bar{\Phi}^a) - J\bar{\Phi}^a)]$$

$$\times \left(\sum_a \exp[-(\Omega/\hbar)('V'(\bar{\Phi}^a) - J\bar{\Phi}^a)] \right)^{-1}. \tag{3.4}$$

Writing $J = J_c + J'$ we obtain.

$$\bar{\Phi} = \sum_a \bar{\Phi}^a \exp[-(\Omega/\hbar)(-J'\bar{\Phi}^a - J_c\bar{\Phi}^a + 'V'(\bar{\Phi}^a))]$$

$$\times \left(\sum_a \exp[-(\Omega/\hbar)(-J'\bar{\Phi}^a - J_c\bar{\Phi}^a + 'V'(\bar{\Phi}^2))] \right)^{-1}. \tag{3.5}$$

Now $-J_c\bar{\Phi}^a + 'V'(\bar{\Phi}^a)$ is the same for all the terms in the summation, so we can divide it out to obtain:

$$\bar{\Phi} = \sum_a \bar{\Phi}^a \exp[-(\Omega/\hbar)J' \cdot \bar{\Phi}^a] \left(\sum_a \exp[-(\Omega/\hbar)J' \cdot \bar{\Phi}^a] \right)^{-1}. \tag{3.6}$$

In these summations the element, or elements, with the largest component in the J' direction will dominate in the infinite volume limit. If $J' \cdot \bar{\Phi}^a$ is maximised for a set of $\bar{\Phi}^a$, denoted by $\{\bar{\Phi}^a\}$ say, then $\bar{\Phi}$, as defined by (2.6), will lie at the centroid of the figure defined by the $\{\bar{\Phi}^a\}$. Although this apparently lies in the non-convex portion of 'V' it has resulted from a linear combination of states of equal energy which are orthogonal in the Hilbert space in the infinite volume limit. It therefore follows that it lies on an interpolated portion of V as shown in § 2.

In conclusion we have shown that $\bar{\Phi}$ will lie at a $\bar{\Phi}^a$, in which case it will be outside a non-convex region or it will lie on an interpolated portion of V. The non-convex portions of 'V' have been excised in the manner suggested by the arguments of Haymaker and Perez-Mercader (1984).

4. Gauge fixing and explicit examples of convexification

Our demonstration of the convexity of V from the properties of $\bar{\Phi}$ depended crucially on the various saddle point contributions being separated. In general with a group G being broken to a (maximal) subgroup H the manifold of minima will be given by G/H and we do not achieve this separation. The remedy, as mentioned in the introduction, is to use an 't Hooft-style gauge fixing term which has the effect of allowing only a discrete set of directions for symmetry breaking in the vector space defined by the Φ's. This picks out a discrete set of allowed points on the manifold of minima. In passing we note that not using such a gauge fixing and cavalierly extending the sum (3.4) to an integral over the group manifold does not appear to affect the behaviour of $\bar{\phi}$, namely that it jumps discontinuously between minima, but one cannot use the approximation $R_a \to R$ to justify the procedure.

We assume a gauge theory with gauge group G, with the Higgs fields in an n-dimensional vector or adjoint representation. The gauge fixing is then

$$-(1/2\alpha)(\partial_\mu A_\mu^\alpha - iT_{ij}^\alpha w_j\phi_i)^2 \tag{1.3}$$

with the w_j an arbitrary vector in Higgs representation space. Consideration of the Nielsen identities (Nielsen 1976, Aitchison and Fraser 1984) for the theory, which guarantee the gauge invariance of physical quantities, then shows that we must have the following condition on the $\bar\phi_i$'s

$$T_{ij}^\alpha w_j\bar\phi_i = 0. \tag{4.1}$$

This will be true in particular on the manifold of minima,

$$T_{ij}^\alpha w_j\bar\phi_{i^0} = 0. \tag{4.2}$$

We now consider separately the vector and adjoint representations of the Higgs fields.

4.1. Vector representation

Taking a real representation first, we note that we can write any $\bar\phi_{i^0}$ on the manifold of minima as a group rotation of some particular $\bar\phi_{i^0}$, say $\bar\chi_i$:

$$\bar\phi_{i^0} = \exp(i\xi_\alpha T^\alpha{}_{ij})\bar\chi_j. \tag{4.3}$$

Thus condition (4.2) can be written as

$$(\partial/\partial\xi_\alpha)(w_j \cdot \bar\phi_{j^0}) = 0. \tag{4.4}$$

Now in a vector representation the manifold of minima will, in general, be a hypersphere as we have only one invariant $\|\bar\phi\|^2$ We can see this by considering

$$\frac{\partial U}{\partial\bar\phi_i} = \frac{\partial U}{\partial\|\bar\phi\|^2} \cdot \frac{\partial\|\bar\phi\|^2}{\partial\bar\phi_i} = 2\phi_i \cdot \frac{\partial U}{\partial\|\bar\phi\|^2} \tag{4.5}$$

which shows that the extrema of U are the local maximum at the origin and the minima on the hypersphere at the radius defined by $\partial U/\partial\|\bar\phi\|^2 = 0$. On this sphere (4.4) will be satisfied for $\bar\chi$ parallel or antiparallel to w, which picks out two antipodal points on the hypersphere. For a complex vector representation we simply write

$$\phi = \phi_1 + i\phi_2 \tag{4.6}$$

with the ϕ_i real and use the gauge fixing term

$$-(1/2\alpha)[\partial_\mu A_\mu^\alpha + (-iT_{ij}^\alpha w_j\phi^+{}_{,i}) + (-iT_{ij}^\alpha w_j\phi^+{}_{,i})^*]^2. \tag{4.7}$$

The argument for the real case is repeated, with the number of components doubled.

4.2. Adjoint representation

For Higgs fields in the adjoint we can write (4.1) as

$$f_{\alpha ij}\bar\phi_i w_j = 0 \tag{4.8}$$

because the T_{ij} are represented by the structure constants $-if_{ij\alpha}$. By making the definitions

$$W = w_j T_j, \qquad \bar\Phi = \bar\phi_j T_j \tag{4.9}$$

(4.8) can be rewritten as

$$[W, \bar{\Phi}] = 0. \tag{4.10}$$

If we now choose W to be a regular element of the algebra (one whose centraliser is the Cartan subalgebra) (4.10) means that $\bar{\Phi}$ is constrained to lie in the Cartan subalgebra. All equivalent minima in $U - J_i\bar{\phi}_i$ are disconnected because, with $\bar{\Phi}$ in the Cartan subalgebra, they are taken into one another by the elements of the Weyl group of G which leave the projection of J onto the Cartan subalgebra invariant. This is a discrete group.

For the vector representations the only critical value of the current is zero and we just consider convexifying between the absolute minima. This is not the case for the adjoint representation, where there may be solutions to $\partial U/\partial \phi = -J_c$ and hence to $\partial^{\cdot} V^{\cdot}/\partial \phi = -J_c$ for values of J_c other than 0.

As an example of this one could consider an SU(3) adjoint potential, though this is not representative in that the relation $(\text{Tr } \Phi^2)^2 = 2 \text{ Tr } \Phi^4$ ensures that the non-convexity vanishes when the quartic terms become dominant. This is not necessarily true in other cases as one can see from consideration of a general adjoint potential at large $\|\phi\|$

$$U(\bar{\phi}) \sim A(\Sigma \bar{\phi}_i^2)^2 + \tfrac{1}{2}A_1(\Sigma \bar{\phi}_i^4). \tag{4.11}$$

The matrix of second derivatives for this

$$\partial^2 U/\partial \bar{\phi}_j \partial \bar{\phi}_k = [4A(\Sigma \bar{\phi}^2) + 6A_1 \bar{\phi}_j^2]\delta_{jk} + 8A\bar{\phi}_j\bar{\phi}_k = U_{jk} \tag{4.12}$$

would be positive semi-definite (which would ensure convexity) only if $v_j U_{jk} v_k \geq 0$ for all v and $\bar{\phi}$. If A were negative, which is allowed by the positivity constraint on the potential, choosing $v = (0, 1, 0 \ldots 0)$ and $\bar{\phi} = (\|\bar{\phi}\|, 0, 0 \ldots 0)$ would give $v_j U_{jk} v_k < 0$, thus showing the potential was non-convex at this point.

Returning to the SU(3) case we could write the SU(3) adjoint potential as (Corrigan *et al* 1976)

$$U(\bar{\phi}) = p(1 - \bar{\phi}^2)^2 + q(\bar{\phi}_i + \sqrt{3}d_{ijk}\bar{\phi}_j\bar{\phi}_k)^2 \qquad p, q > 0 \tag{4.13}$$

after restricting $\bar{\phi}$ to lie in the Cartan subalgebra, λ_3 and λ_8 in the Gell-Mann basis, the potential may be written as

$$U(\bar{\phi}_3, \bar{\phi}_8) = p(1 - \bar{\phi}_3^2 - \bar{\phi}_8^2)^2 + q[\bar{\phi}_3^2(1 + 2\bar{\phi}_8)^2 + (\bar{\phi}_8 - \bar{\phi}_8^2 + \bar{\phi}_3^2)^2]. \tag{4.14}$$
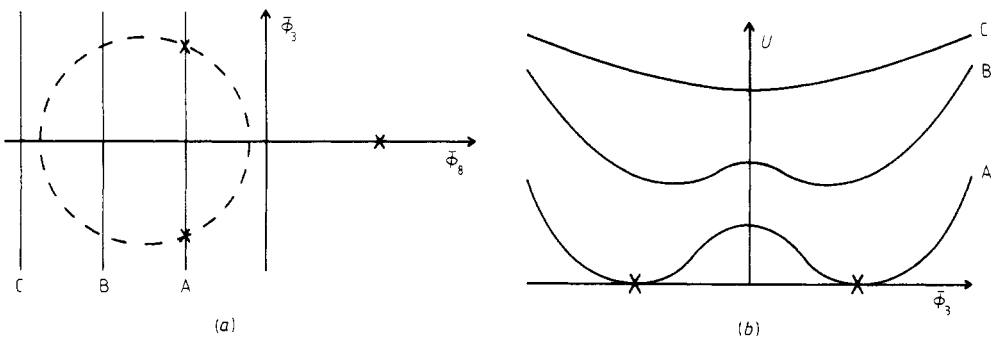
Figure 3. (*a*) The locus of solutions to $\partial U \partial \phi^3 = 0$ is represented by the broken circle. The absolute minima of U are denoted by ×. (*b*) The form of U on the sections *a*, *b*, *c*, in figure 3(*a*).

A plot of $U(\bar{\phi}_3, \bar{\phi}_8)$ shows that there are now other solutions for J_c (see figure 3a). The form of $U(\bar{\phi}_3)$ on three sections A, B, C of figure $3(a)$ is given in figure $3(b)$.

In section B for instance the minima 1, 2 are the solutions to $\partial U/\partial\phi = J$ for some J in the 8 direction and would have to convexify between points 1 and 2. By the time we have reached C the quartic terms are dominant and the non-convexity has disappeared.

In the general adjoint case, the shape of the region to be convexified can be determined for any given direction of J. This is demonstrated in the next section, which also introduces the geometric correspondence between Dynkin diagrams and Coxeter graphs.

5. The geometry of the convexified regions

In the last section we saw that for a vector representation the convexified region was a hypersphere. The adjoint case is now considered. For a scalar field ϕ in the adjoint representation it is known that the Higgs–Kibble mechanism will break the symmetry group G to a maximal compact subgroup with local structure $U(1) \times K$ (Kim 1984). The algebra k of K is obtained by removing a dot from the Dynkin diagram corresponding to the simple root to which $\langle\phi\rangle$ is not orthogonal. In other words $\langle\phi\rangle$ lines up parallel to a fundamental weight (Goddard and Olive 1981a). The elements of K, and in particular the elements of the Weyl group of K, leave $\langle\phi\rangle$ invariant, and so $\langle\phi\rangle$ must lie on the intersection of the hyperplanes normal to the simple roots.

The reflections generated by the broken part of the Weyl group of G will produce a polytope (see appendix) of gauge-equivalent minima of the effective potential obtained by placing a ring around the appropriate nodes in the Coxeter graph corresponding to the Lie algebra of G. For example, $SU(3) \to SU(2) \times U(1)$ gives the polytope ⊙—●, which is a triangle. In fact there are two inequivalent triangles in the root space depending on which node we ring.

SU(4) can break either to $SU(3) \times U(1)$ or $SU(2) \times SU(2) \times U(1)$ and we obtain an octahedron ⊙◄ or a tetrahedron ⊙—●—●. We proceed to enumerate the possible polytopes, subject to the condition that the scalar field lines up parallel to a minimal weight, which ensures the stability against decay of the gauge particle (Goddard and Olive 1981b).

Since G_2, F_4 and E_8 do not have any minimal weights we do not include them.

(i) SU(r)
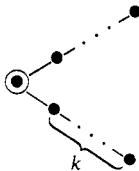
If $k = 0$ we have a regular $(r-1)$ simplex, written α_r. The general figure consists of taking the centroids of all the constituent k simplices as the vertices of the new polytope.

In $SU(5) \to SU(3) \times SU(2) \times U(1)$, $k = 1$, and we take the centres of the edges of the 4-simplex; its projection onto a plane (see figure 4).
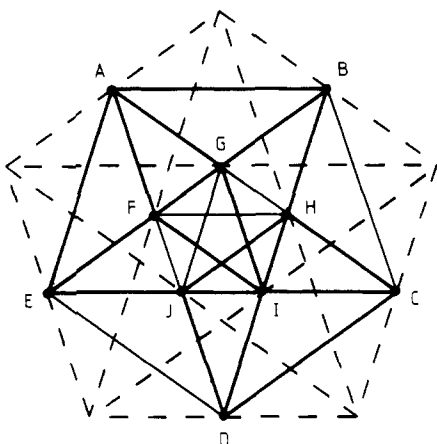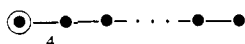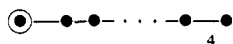
Figure 4. A projection of $\{^3_{3,3}\}$ onto a plane, the polytope produced by the minima of the potential in $SU(5) \rightarrow SU(3) \times SU(2) \times U(1)$.
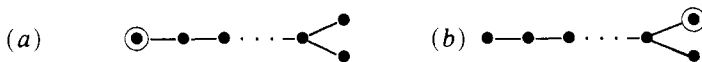
(ii) $SO(2r+1)$

The only minimal weight is the one on the end of the double link. Hence the only shape produced is the hypercube, written γ_r.
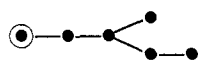
(iii) $Sp(r)$

The only minimal weight for this group is at the other end; this is the notation for β_r, or the cross-polytope, which consists of vertices at $(\pm a, 0, \ldots, 0)$ and permutations.
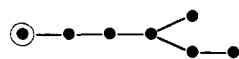
(iv) $SO(2r)$

(a) (b)

(a) is again just a cross-polytope β_r, while (b) is the partial truncation of γ_r, written $h\gamma_r$, obtained by eliminating half of the points on it. Clearly $h\gamma_3$ is α_3.

(v) E_6

This is termed Gosset's regular figure in six dimensions, which is bounded by 72 6-simplexes (α_5) and 27 five-dimensional cross polytopes (β_5).

(vi) E_7

This is Gosset's seven-dimensional regular figure, and is bounded by 56 of the previous figures and 576 α_6's.

We now know the shapes in the Cartan subalgebra of the degenerate minima of the effective potential at $J = 0$. Simple forms of the coordinates of α_r, β_r, γ_r and $h\gamma_r$

are given in the appendix. The argument supposes that 'V' calculated to some order in the loop expansion breaks G to a maximal compact subgroup H, but we can extend it if higher-order radiative corrections break H further. For example, if SU(3) → U(1) × U(1) then the Weyl group of SU(3) is completely broken, and the polytope is ⊙—⊙, which is just the semi-regular hexagon obtained by reflecting a point inside the positive Weyl chamber. We shall assume for simplicity that H is unbroken beyond first order, but the extension to a general subgroup of G should be apparent.

Our gauge-fixing procedure has reduced the manifold of minima of 'V' to the centraliser of W, the adjoint gauge-fixing vector, which is by definition the Cartan subalgebra if W is regular. Thus from the results of § 2 the interpolated region must lie within or on the boundary of the polytope formed by the degenerate minima. At $J = 0$ this is just obtained by ringing one of the nodes of the Coxeter graph, as we saw in § 4, but there are other values of J for which the ground state is degenerate. That is,

$$(\partial/\partial\Phi)('V' - \mathrm{Tr}(J\bar{\Phi})) = 0 \tag{5.1}$$

has more than one solution for $J = J_c$. This can happen in either of two ways. Firstly, consider SU(4) → SU(3) × U(1). Let J be very small and opposite to the outward normal to one of the faces of the tetrahedron (J_1 in figure 5). Then there will be a triangle {123} of degenerate minima of 'V' − $\mathrm{Tr}(J\bar{\Phi})$. If $\mathrm{Tr}(J\bar{\Phi}_1) = \mathrm{Tr}(J\bar{\Phi}_2)$, as it does for J_2, then there will be degenerate minima {34} and {12}.

Thus if J is invariant under the action on the Weyl group of one of the elements Π_k of a polytope Π_n, the degeneracy between the vertices of that element will not be lifted, and the convexified region will be the convex hull of the solutions of (5.1), which will be the boundary and interior of a polytope Π_k. In the previous example the tetrahedron is ●—●—● and J_1 is invariant under the automorphisms of a ●—●, while J_2 is invariant under the interchange of the ends of an edge ●. Hence the convexified regions of 'V' − $\mathrm{Tr}(J\bar{\Phi})$ are a triangle and a line element respectively. As we increase the magnitude of J the polytope of the remaining degenerate minima Π_k will move away from the origin in the field space. For SU(3) it eventually vanishes in size (line c in figure 3a), but as we showed in the last section this is the exception rather than the rule: regions of non-convexity may in general extend to infinity, so that Π_k never disappears.

There is also the possibility that for certain values of the parameters of the potential there may be a local minima which break the symmetry in another way, which also
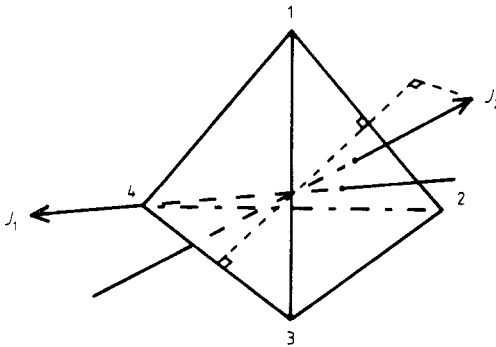
Figure 5. The tetrahedron of minima for SU(4) → SU(3) × U(1) showing two possible currents that leave some of the minima degenerate (see text).

have associated regions of non-convexity. For example, for some values of the parameters in an SU(5) potential there may be SU(4) × U(1) local minima which become absolute minima for certain values of *J*. However, the convexification of the absolute minima will not be affected, but in general we would expect the shapes of the regions of non-convexity to become more complicated.

Hence we have a general procedure for convexifying '*V*' everywhere.

(1) Find those $\bar{\Phi}$ for which (5.1) has more than one solution for some value of *J*.

(2) Linearly interpolate '*V*' between these points, which will form the vertices of a polytope somewhere in the field space, so that everywhere in this region *V* will take the same value as at the vertices.

The converse procedure, finding $V(\bar{\Phi})$ for some $\bar{\Phi}$, is not easy, as it demands finding the minima of 'V' $- \mathrm{Tr}(J\bar{\Phi})$ on whose convex hull $\bar{\Phi}$ lies, and we do not attempt it here. In general, as shown in § 4, the regions of non-convexity may extend to infinity and change in size but the shapes will always be the same as the cells to which they tend as $J \to 0$.

6. Conclusion

In this paper we have shown that it is possible to produce a convex effective potential to any desired order using the interpolated loop expansion with the Higgs fields in a vector or adjoint representation. This extends the results of Fujimoto *et al*, who considered only a single scalar field, and we find that in order to make sense of their procedure it is necessary to treat the scalar fields as a sector in a gauge theory and use the consequent freedom to fix the gauge to limit the minima of the effective potential to a finite number of separate points. Using the equivalence of Dynkin diagrams and Coxeter graphs we find that the convexified regions form regular convex polytopes when the scalar fields are in the adjoint representation and that they form hyperspheres when in a vector representation. These regions are to be interpreted as quantum superpositions of the separate ground states at zero temperature.

Appendices

We summarise as briefly as possible the results about regular polytopes that may be found in Coxeter (1948), and show that gauge-equivalent minima of the effective potential of adjoint scalars form exactly these shapes in the Cartan subalgebra. Since the Coxeter graphs for regular polytopes and the Dynkin diagrams for Lie algebras of rank *r* are derived in similar ways (from considerations of reflection symmetries in S^r) this is no surprise, but it is convenient here to make the connection and to present the results together in one place.

Appendix 1. Regular polytopes

Polytopes are regular figures in n dimensions. When $n = 0, 1, 2, 3$ they are respectively points, line segments, polygons and polyhedra if they are finite. If they are infinite they are Euclidean lattices or honeycombs. Clearly, regular figures will have certain reflection symmetries, and it is by the various possible symmetry groups that they are classified. We will restrict ourselves to convex polytopes in this discussion, as the stellated ones (which occur in up to four dimensions) are not relevant—the group transformations on the scalar field leave its length invariant. The finite polytopes must be generated by reflections in a finite space, so what we do is consider 'inflated' n-dimensional polytopes Π_n lying on an $(n-1)$ sphere, and points on this sphere are reflected in great $(n-2)$ spheres. These 'mirrors' divide the sphere into fundamental regions, which are n simplexes—in fact they form a tessellation of the $(n-1)$ sphere (see figure A1). The number of these fundamental regions is equal to the order of the underlying reflection group. Placing a point on the sphere will generate a regular figure from its reflections, the most symmetric figures being obtained by placing it at the intersection of all but one of the mirrors, so that the resulting polytope will have all but one of the symmetries.
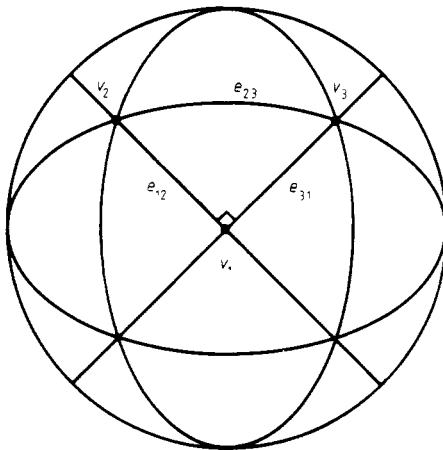
Figure A1. Tesselation of the 2-sphere by fundamental regions v_1, v_2, v_3. Reflections of v_1 generate an octahedron; reflections of v_2 and v_3 generate tetrahedra.
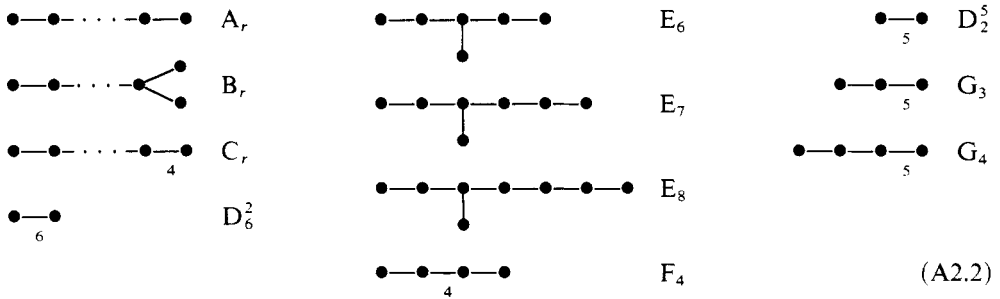
Appendix 2. Coxeter graphs and Dynkin diagrams

The reflection symmetries created by this spherical tessellation may be represented by Coxeter graphs, where the nodes stand for mirrors and the connecting numbered branches the angles between them. If the nodes are not connected the mirrors are orthogonal. A typical graph might be

$$\underset{p \quad\ q \quad\ r \quad\ s}{\bullet\!\!-\!\!\bullet\!\!-\!\!\bullet\!\!-\!\!\bullet\!\!-\!\!\bullet} \qquad\qquad (\text{A2.1})$$

where the angles between the mirrors are π/p, π/q, etc. If the number is 3 it is omitted.

By considering the geometrical properties of the normals to the mirrors (analogously to the roots of a Lie algebra) it is possible to show that the only spherical tessellations are as follows[†]:

$$\bullet\!-\!\bullet\!-\cdots-\!\bullet\!-\!\bullet \quad A_r \qquad\qquad \bullet\!-\!\bullet\!-\!\bullet\!-\!\bullet\!-\!\bullet \quad E_6 \qquad\qquad \bullet\!\underset{5}{-}\!\bullet \quad D_2^5$$

$$\bullet\!-\!\bullet\!-\cdots-\!\!\!\!<^{\bullet}_{\bullet} \quad B_r \qquad\qquad \bullet\!-\!\bullet\!-\!\bullet\!-\!\bullet\!-\!\bullet\!-\!\bullet \quad E_7 \qquad\qquad \bullet\!-\!\bullet\!\underset{5}{-}\!\bullet \quad G_3$$

$$\bullet\!-\!\bullet\!-\cdots-\!\bullet\!\underset{4}{-}\!\bullet \quad C_r \qquad\qquad \bullet\!-\!\bullet\!-\!\bullet\!-\!\bullet\!-\!\bullet\!-\!\bullet\!-\!\bullet \quad E_8 \qquad\qquad \bullet\!-\!\bullet\!-\!\bullet\!\underset{5}{-}\!\bullet \quad G_4$$

$$\bullet\!\underset{6}{-}\!\bullet \quad D_6^2 \qquad\qquad \bullet\!-\!\bullet\!\underset{4}{-}\!\bullet\!-\!\bullet \quad F_4 \qquad\qquad\qquad (A2.2)$$

The similarity with the Dynkin diagrams for the generators of compact simple Lie groups is obvious. This is because the Weyl reflections in the hypersurfaces normal to the simple roots of the algebra generate these finite reflection groups in exactly the same way. With the Lie algebras the lengths of the roots are important (as the roots are derived from the structure constants), and so we distinguish between $SO(2r+1)$ and $Sp(r)$, whose roots generate the symmetry

$$\bullet\!-\!\bullet\!-\cdots-\!\bullet\!\underset{4}{-}\!\bullet. \qquad\qquad (A2.3)$$

The interesting exceptions to the equivalence are the three tesselations D_2^5, G_3 and G_4, which as far as we are aware do not correspond to any known algebra.

Appendix 3. Wythoff's construction of the regular polytopes

Referring to figure A1, we see that placing a point at v_2 will produce a tetrahedron after reflection. We represent this by placing a ring around the node representing the mirror which it is *not* on, so that a tetrahedron is

$$\circledcirc\!-\!\bullet\!-\!\bullet \qquad\qquad (A3.1)$$

while an octahedron is

$$\circledcirc\!\!\!<^{\bullet}_{\bullet}. \qquad\qquad (A3.2)$$

If the point is somewhere inside the fundamental region we write

$$\circledcirc\!-\!\circledcirc\!-\!\circledcirc. \qquad\qquad (A3.3)$$

However, these figures will turn out not be of interest in the context of symmetry breaking in the adjoint representation. There is an alternative notation for these polytopes by Schlafli which are for the tetra- and octahedron $\{3, 3\}$ and $\{^3_3\}$ respectively. If we were to place a ring around an inner node in one of the exceptional groups,

[†] Note that this is Coxeter's notation, which differs slightly from the usual Lie algebra designations; in particular his B_r is usually written D_r, his C_r is usually B_r, and his D_2^6 is more often G_2.

then we might get

$$
\text{⊙} \mathrel{<\!\!\!\cdot} \cdots \bullet\!\!-\!\!\bullet = \left\{ \begin{matrix} & 3 \\ 3 & \\ & 3,\ 3 \\ 3 & \end{matrix} \right\}. \tag{A3.4}
$$

This eight-dimensional figure will also turn out not to be important for our purposes. The meaning of the symbol $\{p, q\} = \text{⊙}\!\!-\!\!\underset{p}{\bullet}\!\!-\!\!\underset{q}{\bullet}$ is fairly straightforward: it is the polyhedron with q faces at each vertex, each of which is a $\{p\}$. So for example an octahedron may be written $\{3, 4\}^\dagger$. The reciprocal figure $\{4, 3\} = \text{⊙}\!\!-\!\!\underset{4}{\bullet}\!\!-\!\!\underset{3}{\bullet}$ is just a cube, which is obtained by joining the centroids of the faces of the octahedron. We can obtain another polyhedron $\left\{ \begin{matrix} p \\ q \end{matrix} \right\} = \text{⊙} \mathrel{<} \!\!\!\overset{\underset{p}{\bullet}}{\underset{q}{\bullet}}$ by joining the centres of the edges of the polyhedron, so that each vertex is replaced by a $\{q\}$. Then if $p = 3$ and $q = 4$, $\{^3_4\} = \{^4_3\}$ is a cuboctahedron, pictured in figure A2. A polytope Π_n, whose Coxeter graph is

$$
\text{⊙}\!\!-\!\!\underset{p}{\bullet}\!\!-\!\!\underset{q}{\bullet}\!\!-\!\cdots-\!\!\underset{s}{\bullet}\!\!-\!\!\underset{t}{\bullet}\!\!-\!\!\underset{u}{\bullet}\!\!-\!\cdots-\!\!\underset{x}{\bullet} = \{p, q, \ldots, s, t, u, \ldots, x\} \tag{A3.5}
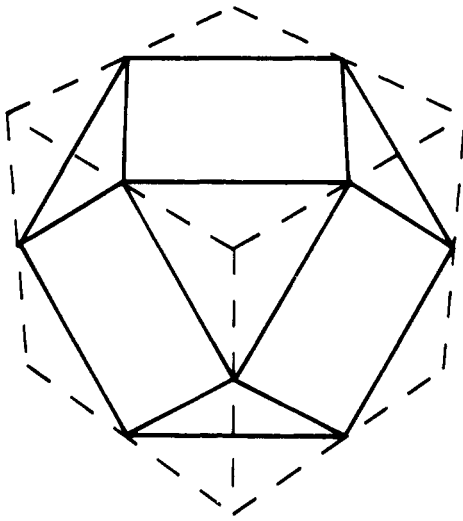$$

Figure A2. A cuboctahedron, the figure obtained by joining the midpoints of the edges of a cube (or an octahedron).

contains a number of $\{p, q, \ldots, s\}$'s. If we construct another polytope whose vertices are the centroids of these figures we obtain

$$
\text{⊙} \mathrel{<} \!\!\!\overset{\underset{t}{\bullet}\!\!-\!\!\underset{s}{\bullet}\!\!-\!\cdots-\!\!\underset{q}{\bullet}\!\!-\!\!\underset{p}{\bullet}}{\underset{u}{\bullet}\!\!-\!\cdots-\!\!\underset{w}{\bullet}\!\!-\!\!\underset{x}{\bullet}} = \left\{ \begin{matrix} t, s, \ldots, q, p \\ u, \ldots, w, x \end{matrix} \right\}. \tag{A3.6}
$$

---

† This is a consequence of the embedding of $SO(2r)$ in $SO(2r+1)$. In general, any figure containing a fishtail will be the same as one with the three nodes of the tail replaced by $\cdots-\!\!\bullet\!\!-\!\!\bullet\!\!-\!\!\underset{4}{\bullet}$

This operation is called truncation, and the resulting polytope contains, analogously to the polygonal faces of the polyhedron, the $(n-1)$-dimensional boundary cells

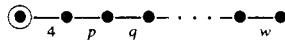$$\text{(diagram)} \quad \text{and} \quad \text{(diagram)} \tag{A3.7}$$
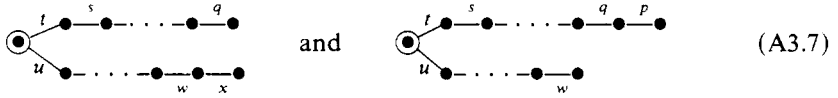
The elements that bound these cells in turn (which will be Π_{n-2}'s) may be obtained by removing a node and a branch, working from the right.

The polytope

$$\text{(diagram)} \tag{A3.8}$$

is a so-called partial truncation of

$$\text{(diagram)}$$

obtained by removing alternate vertices. This can be done unambiguously, as every face $\{4\}$ has an even number of sides, and every circuit in the polytope can be tiled with $\{4\}$'s. As a trivial example, the tetrahedron $\circledcirc\!\!-\!\!\bullet\!\!-\!\!\bullet$ is a partial truncation of the cube $\circledcirc\!\!-\!\!\underset{4}{\bullet}\!\!-\!\!\bullet$.

It is possible to work out how many elements Π_k, $0 \leq k < n$, of a particular type are contained within a polytope. For example, consider an $(n+1)$ simplex

$$\text{(diagram)} \tag{A3.9}$$

Suppose we wish to find out the number of triangles $\circledcirc\!\!-\!\!\bullet$ in it. Each triangle will be left invariant under a reflection subgroup W_{n-3}, because the normals of the mirrors are orthogonal to the plane of the triangle. The subgroup W_2 just takes the triangle into itself. Thus the number of triangles in an $(n+1)$ simplex is (reading off the orders of the reflection groups from table A1)
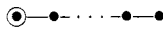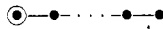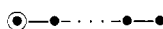
$$O(W_n)/[O(W_2)O(W_{n-3})] = (n+1)!/[3!(n-2)!] \tag{A3.10}$$

where $O(W)$ denotes the order of the Weyl group. The general procedure for calculating which and how many of a certain element there are is to remove up to f nodes from

Table A1

Tesselation	Order
A_r	$(r+1)!$
B_r (D_r)	$2^{r-1}r!$
C_r (B_r)	$2^r r!$
E_6	$72 \times 6!$
E_7	$8 \times 9!$
E_8	$192 \times 10!$
D_2^6 (G_2)	12
F_4	1192

Table A2

Coexeter graph	Name	
	$(r+1)$ simplex	α_r
	cross-polytope	β_r
	hypercube/measure polytope	γ_r

a graph with f free ends, and then factor out the remaining Weyl groups as above. For example, in (A3.4) we can obtain two sorts of triangles

 and (A3.11)

where the open circles indicate the removed nodes.

A useful check to see if all the elements of a polytope have been obtained is Euler's formula

$$\sum_{i=0}^{n-1} N_i = 1 - (-1)^n. \tag{A3.12}$$

The three simplext finite regular convex polytopes are listed in table A2. Table A3 displays cartesian coordinates for the regular convex polytopes derivable from them by truncation. Note that, although it is easiest to write down the coordinates for the figures derived from α_r in $\mathbb{R}^{r+1}$, we can rotate them into an $\mathbb{R}^r$ subspace by the following procedure (v is a vertex).

(1) $\qquad v \rightarrow v' = v - (1/(r+1), \ldots, 1/(r+1))$

(2) $\qquad v' \rightarrow v'' = M_2 M_1 v'$

$$M_1 = \begin{bmatrix} 1 & 0 & \cdots & 0 \\ 0 & r^{-1/2} & \cdots & r^{-1/2} \\ \vdots & \vdots & & \vdots \\ 0 & r^{-1/2} & \cdots & r^{-1/2} \end{bmatrix}$$
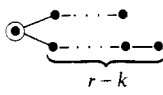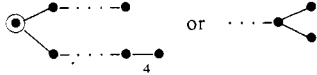
If r is odd:

$$M_2 = \begin{bmatrix} [r/(r+1)]^{1/2} & 0 & \cdots\cdots & 0 & (r+1)^{-1/2} \\ 0 & 2^{-1/2} & 0 & \cdots & 0 & 2^{-1/2} & 0 \\ \vdots & & 0 & \ddots & & 0 & \vdots \\ \vdots & \vdots & & 2^{-1/2} & 2^{-1/2} & & \vdots \\ \vdots & \vdots & & 1 & & \vdots \\ \vdots & \vdots & & 2^{-1/2} & 2^{-1/2} & & \vdots \\ \vdots & & 0 & \ddots & & 0 & \vdots \\ 0 & -2^{-1/2} & 0 & \cdots & 0 & 2^{-1/2} & 0 \\ -(r+1)^{-1/2} & 0 & \cdots\cdots & 0 & [r/(r+1)]^{-1/2} \end{bmatrix}.$$

If $r+1$ is even the matrix is as before except that the figure 1 is removed from the centre.

Table A3

Coxeter graph (r nodes)	Coordinates
	$(\overbrace{1,\ldots,1}^{k},0,\ldots,0)+{}^{r+1}C_k$ perms (in $\mathbb{R}^{r+1}$)
or	$(\pm 1,\ldots,\pm 1,0,\ldots,0)+{}^{r}C_k$ perms
	$(\pm 1,\ldots,\pm 1)\left.\begin{array}{l}\text{odd}\\ \text{even}\end{array}\right\}$ **number of $-$signs**

References

Aitchison I J R and Fraser C M 1984 *Ann. Phys., NY* **156** 1

Callaway D J E and Maloof D J 1983 *Phys. Rev.* D **27** 406

Corrigan E, Olive D, Fairlie D B and Nuyts J 1976 *Nucl. Phys.* B **106** 475

Coxeter H S M 1948 *Regular Polytopes* (London: Methuen)

Do Amaral M G, De Carvalho C A A and Shellard R C 1984 *Revista Bras. Fis.* **14** 24

Evans M and McCarthy J 1984 *Preprint, On the Quantum Mechanics of Inflation* RU84/B/ Rockefeller University

Fujimoto Y, O'Raifeartaigh L and Parravicini G 1983 *Nucl. Phys.* B **212** 268

Fukuda R 1976 *Prog. Theor. Phys.* **56** 258

Goddard P and Olive D 1981a *Nucl. Phys.* B **191** 511

—— 1981b *Nucl. Phys.* B **191** 528

Glimm J and Jaffe A 1981 *Quantum Physics, a Functional Integral Point of View* (Berlin: Springer)

Haymaker R W and Perez-Mercader J 1983 *Phys. Rev.* D **27** 1948

Iliopoulous J, Itzykson C and Martin A 1975 *Rev. Mod. Phys.* **47** 165

Jackiw R 1974 *Phys. Rev.* D **9** 1686

Kim J S 1984 *J. Math. Phys.* **25** 1694

Nielsen N K 1975 *Nucl. Phys.* B **101** 173